Journal Pre-proofs

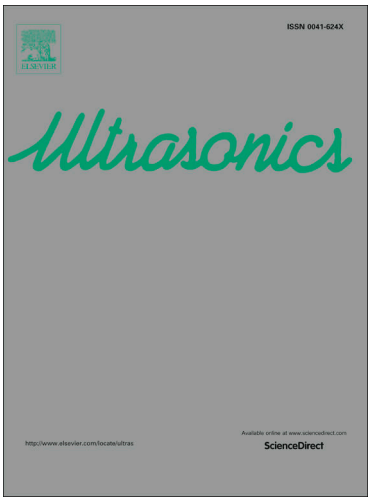

Acoustic field visualisation using local absorption of ultrasound and thermochromic liquid crystals

O. Trushkevych, M. Turvey, D.R. Billson, R. Watson, D.A. Hutchins, R.S. Edwards

PII: S0041-624X(24)00062-3
DOI: https://doi.org/10.1016/j.ultras.2024.107300
Reference: ULTRAS 107300

To appear in: *Ultrasonics*

Received Date: 3 October 2023
Revised Date: 15 March 2024
Accepted Date: 16 March 2024

Please cite this article as: O. Trushkevych, M. Turvey, D.R. Billson, R. Watson, D.A. Hutchins, R.S. Edwards, Acoustic field visualisation using local absorption of ultrasound and thermochromic liquid crystals, *Ultrasonics* (2024), doi: https://doi.org/10.1016/j.ultras.2024.107300

Acoustic field visualisation using local absorption of ultrasound and thermochromic liquid crystals

O. Trushkevych[1,2*], M. Turvey[2], D.R. Billson[1], R. Watson[1], D.A. Hutchins[1] and R.S. Edwards[2†]

[1]School of Engineering and [2]Department of Physics, University of Warwick, Coventry CV4 7AL, UK

Abstract

Acoustic field and vibration visualisation is important in a wide range of applications. Laser vibrometry is often used for such visualisation, however, the equipment has a high cost and requires significant user expertise, and the method can be slow, as it requires scanning point by point. Here we suggest a different approach to visualisation of acoustic fields in the kHz – MHz range, using paint-on or removable film sensors, which produce a direct visual map of ultrasound displacement. The sensors are based on a film containing thermochromic liquid crystals (TLC), along with a backing/underlay layer which improves absorption of ultrasound. The absorption generates heat, which can be seen by a change in colour of the TLC film. A removable sensor is used to visualise the resonant modes of an air-coupled flexural transducer operated from 410 kHz to 7.23 MHz, and to visualise 40 kHz standing waves in a Perspex plate. The thermal basis of the visualisation is confirmed using thermal imaging. The speed and cost of visualisation makes the new sensor attractive for use in condition monitoring, for fast assessment of transducer quality, or for analysis of acoustic field distribution in power ultrasonic systems.

1. Introduction

Ultrasound is commonly used in many applications, from medical inspection and treatment through to non-destructive testing (NDT). In each field, quick and effective ways to visualise ultrasound fields are necessary. For example, in the aerospace, automotive and electronics industries, visualisation of how ultrasound travels in the vicinity of defects can help to develop new condition monitoring and NDT techniques and aid understanding of how sound interacts with defects [1]. In materials research and development, as well as for high power industrial ultrasonics, and medical diagnostic / therapeutic ultrasound, imaging of the wavefield generated by the transducers used can ensure that they are effective and operating at the correct frequency. This requires measurements to be done on the transducer and in the air to measure e.g. focal points and vibration frequencies [2].

The gold standard for visualisation of ultrasound and vibration is currently laser vibrometry [3,4,5], where a laser beam is scanned over the sample surface and the displacement or velocity of the surface is measured at each position. Laser vibrometry offers high lateral resolution and sensitivity to nm displacements, however, the cost is high, and the point-by-point scanning puts limitations on the measurement speed. Current commercial systems can probe vibrations with frequencies of up to 2.4 GHz, but measurements at higher frequencies are difficult, and systems operating above 1 MHz are significantly more expensive. Vibrometry measurements are conducted on the surface of a sample, with some constraints on surface finish, and the technique is not suitable for testing beam profiles in air. Hydrophones or microphones can be used singly or in arrays for point-by-point scanning, for measurements in air or water. These have limited lateral resolution due to the microphone size, and so are not always suitable.

A third method of ultrasound mapping is acoustography, which has been developed to map ultrasonic fields in a water bath [6]. The sensitive element is a layer of aligned nematic liquid crystal (LC) held between crossed polarisers [7]. For NDT measurements, a sample can be placed between a transducer generating ultrasound plane waves and the LC sensor, which changes optical properties depending on the amplitude of ultrasound reaching each point on the sensor. This gives a visual image of how the ultrasound has propagated through the material, indicating the presence of defects by shadows in blocked regions, in a similar manner to radiography. The technique allows imaging over an area of several cm^2, and when compared to conventional ultrasonic scans (C-scans), it has been reported to have higher resolution, offering almost real-time imaging speed, and comparable [8-10] or superior defect detection

* o.trushkevych@warwick.ac.uk
† r.s.edwards@warwick.ac.uk

capability [11]. However, acoustography requires a setup with ultrasound at oblique incidence to the sensor, and is currently limited to operation at 3.3 MHz, and must be done in a water bath, limiting sample size.

Thin film removable sensors and paint-on ultrasound sensors which can give an image of ultrasound wavefields similarly to acoustography are an attractive concept for a variety of applications, particularly for wavefield imaging, as they would offer a much simpler inspection, without the need for a water bath. Earlier research has developed film sensors based on nematic LC droplets dispersed in a polymer film, which could be applied to a material for imaging ultrasound vibrations [12-14]. In these materials, the LC has a different refractive index depending on whether or not it is aligned, and the polymer's refractive index is chosen to match that of the aligned LC state. An applied field such as ultrasound can turn the film from scattering (unaligned) to clear (aligned), leading to cleared regions on the sensor where the ultrasound amplitude is sufficient to align the LCs within the droplets. These polymer dispersed LC films (PDLC) were demonstrated to visualise displacement patterns of an air-coupled ultrasound transducer at 320 kHz – 10 MHz when placed onto the transducer. However, the dynamic range of the film is small, with almost on-off switching characteristic, and increased sensitivity is required.

A different class of LC called thermochromic liquid crystals (TLC) offers potential for improved thin film sensors [15]. These materials display a temperature-dependent structural colour, and are used extensively in simple visual forehead thermometers. The colour comes from the helical structure into which the molecules in the LC state assemble. Light is selectively reflected from the helix (Bragg diffraction), and as the helical pitch changes with temperature, so does the colour of the TLC. The helical pitch and the temperature range in which it scatters light in the visible range can be controlled by careful choice of the composition of the LC mixture. TLC sheets for temperature mapping are commercially available for a variety of temperature ranges [16]. The sheets contain droplets of TLC that are encapsulated and embedded into a polymer sheet with a black background for contrast. Water based paint-on TLC inks are also available [17].

The use of TLC for mapping ultrasound was first explored in the 1970s [18-21], mainly for ultrasound beams in a water bath, with applications limited as TLC-loaded polymer sheets had not been developed. The TLC layer was painted onto a bath window, or TLC-coated plates were placed inside the water bath. In the late 1970s research on using LCs to map ultrasound shifted towards using nematic LCs [21], because nematic LCs, being directly sensitive to pressure, were more sensitive in the water bath arrangements used at the time, leading to the development of acoustography [22]. TLCs have been revisited more recently for beam profile mapping, again in water baths [23,24,25], with similar measurements performed using plates with thermochromic dye (not TLC) [26,27]. The mechanism behind the ultrasound visualisation in TLC is thermal. Local absorption of ultrasound in the TLC film leads to vibrational energy being converted to heat, with the local heating visible as a colour change. When the TLC film is placed in a water bath, water's high thermal conductivity reduces the thermal contrast significantly, and hence this is a very ineffective way of operating a TLC sensor. This may explain why the technology has not become widely used.

In this work we apply a new, removable film sensor, based on a TLC film with an absorbing underlay to a variety of samples. The resonances of an air-coupled flexural transducer are imaged over a wide frequency range, with the thermal basis of the imaging confirmed by applying just the absorbing underlay to the transducer and using thermal imaging. In addition, operation at very low ultrasonic frequencies (40 kHz) is demonstrated by imaging standing waves in a thin Perspex plate. The new sensor is removable and reusable, offering an alternative to the current expensive and slow methods for wavefield imaging, with the potential to be used on a sample or in air or water.

2. Methodology

Compound sensors were produced by adhering the TLC film to an elastic underlay (backing layer) which improved energy absorption, and ensured that the film had sufficient sensitivity to the ultrasound displacements used. TLC films are available commercially with different operating temperatures and sensitivity range, and a suitable underlay was chosen following tests of different commercially available materials. A set of differently sized compound sensors were produced, with the size dependent on the application. TLC films operating over a temperature range of 25-30^{o}C were obtained from Eliott Scientific, with the sheet changing from red to blue over this temperature range with a black background to provide contrast. This was chosen to enable detection at room temperature, with a sensitivity range suitable for the expected amount of heating due to absorption of ultrasound. Note that room temperature was around 21°C but was not strictly controlled, to ensure conditions

matched those in which the sensors would be used. Each sensor is removable and reusable.

The films were placed onto several different samples in order to demonstrate different applications. A flexural ultrasound transducer with a fundamental resonance mode at 40 kHz was used as a generator in order to test the sensitivity of the compound sensor to ultrasonic vibrations of different frequencies. This was operated over a frequency range of 320 kHz – 10 MHz, which offered a set of higher order resonant modes with interesting vibration patterns. The transducer contained a 9 mm diameter piezoelectric element glued onto an aluminium cap which was 25 mm in diameter [28]. The transducer was excited by a continuous sine wave using a function generator and a 25 W RF power amplifier. Imaging of higher frequency vibrational modes of this transducer using a laser vibrometer and a nematic LC based film sensor was reported earlier [12, 13]. TLC films with and without underlay were coupled to the face of the flexural transducer with ultrasound coupling gel (Ultragel). A schematic of the set-up is given in figure 1(a). Measurements were also performed with the elastic underlay applied directly to the transducer face without TLC film. For this set-up the heat generation in the underlay was measured directly using a Cedex Titanium 20 thermal camera with 320x240 pixels resolution and 0.1K sensitivity.

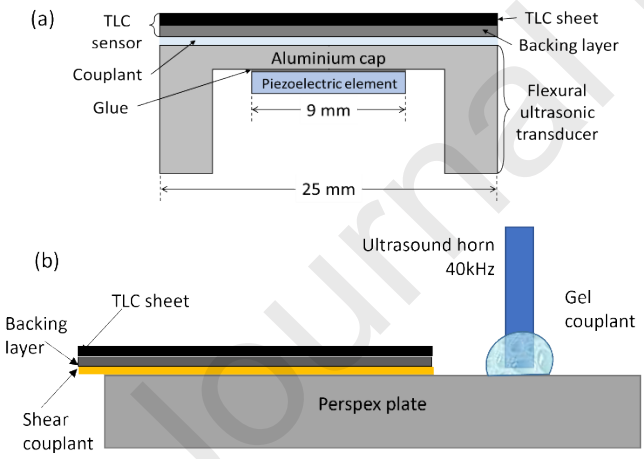

Figure 1: Experimental set-ups for the compound sensor, for (a) measurement of the vibrations of a flexural ultrasound transducer, and (b) measuring standing waves on a Perspex plate.

The resonances of the flexural transducer were analysed using a finite element model (FEM, using PZFlex) and an Intelligent Optical Systems (IOS) two-wave mixer interferometer pointed at the centre of the transducer, in order to measure the expected displacements of all modes. The model data was taken from the sum of the Fourier transforms for a line of elements across the centre of the transducer and will show asymmetric and axisymmetric modes, while only axisymmetric modes where there is significant displacement at the centre would have been captured by the interferometer. Results from both are shown in figure 2, where a series of peaks show that the amplitude of the displacement varies depending on the mode and the frequency with higher amplitudes generally observed at lower frequencies. A Polytec laser vibrometer was also used to map one of the high order modes of the flexural transducer without the compound sensor in place, to confirm the displacement behaviour pattern observed.

For low frequency experiments, an ultrasonic horn 40 kHz (Sonics Ltd.) with a power supply unit was used (figure 1(b)). This was applied to a 3mm thick Perspex plate in order to generate Lamb waves [29]. The horn was placed in different positions on the plate and was recoupled using ultrasound gel for each position. The compound sensor formed from a TLC sheet with elastic underlay was coupled to the Perspex plate using shear couplant, so that both the out-of-plane and in-plane displacement characteristic of Lamb waves was coupled into the TLC sheet. The compound sensor was placed so that the sensor protruded over the edges of the plate.

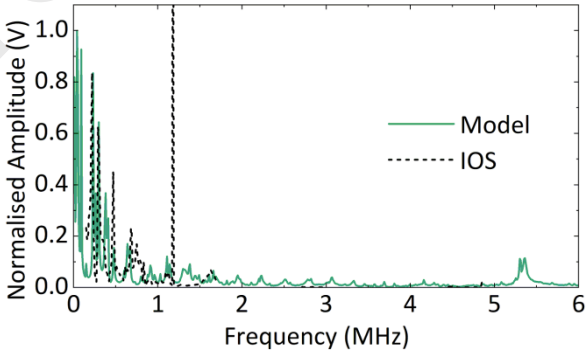

Figure 2: Resonant frequencies of flexural transducer measured by laser interferometer and calculated using FEM.

3. Results and discussion

Figure 3 shows imaging of the 720 kHz, 11:0 vibrating plate mode of the transducer using different techniques. Figure 3(a) shows a measurement using the laser vibrometer, scanned across the face of the transducer, which took around 8 hours to complete (previously reported in [12]). The vibrational pattern is shown as a number of rings of higher displacement amplitude, with yellow representing the largest positive amplitude (peaks) and dark blue the largest negative amplitude (troughs). There are 6 peaks and 5 troughs, hence 11 nodes. The central spot has the largest amplitude. Imaging using the vibrometer allows the positive and

negative vibration amplitudes to be distinguished, whereas the compound sensor only images the magnitude of the vibration, leading to the positive and negative resonance rings both showing as bright rings. Figure 3(b) shows the same mode imaged using the removable compound TLC sensor placed onto the transducer and coupled using gel. Again, a series of rings are observed, with the largest amplitude shown for the central spot. As the TLC sensor measures the magnitude of the displacement rather than absolute value, the maxima and minima both are shown as 11 bright rings. Non-uniformity of the rings is observed for both images. This is due to mode mixing with nodal-line modes, and non-uniformity of the transducer due to variability of the cap thickness and piezoelectric element, with the largest contribution likely to come from the irregularities of the glue bond between them [30].

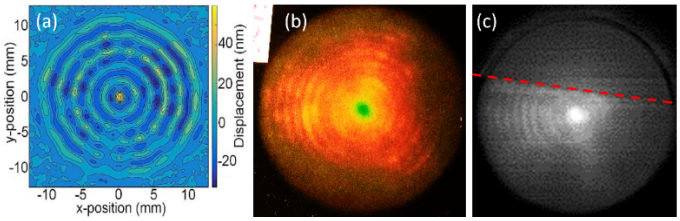

Figure 3: 720 kHz (vibrating plate mode 11:0) resonance of the air coupled transducer with 25mm diameter, driven at 1W, imaged using (a) laser vibrometer measurement (8-hour scan); (b) TLC sensor on the transducer, with elastic film underlay, coupled with ultrasound gel (2 s); (c) Thermography, with transducer coated with black paint for even IR emissivity, with the section below the dashed line covered with the elastic underlay.

Photographs showing the sensing capabilities of TLC sensor with backing when placed on a flexural transducer, for a variety of frequencies from 410 kHz to 7.23 MHz, are given in figure 4. Circular patterns covering the whole face of the transducer were observed at all frequencies, although some wavemodes had a much stronger pronounced central displacement, such as the mode shown in figure 5(b). This contrasts with our work on PDLC [13,14], where only the central displacement could be visualised at frequencies above 1 MHz; this is due to the increased sensitivity of the TLC compound sensor when using a suitable underlay.

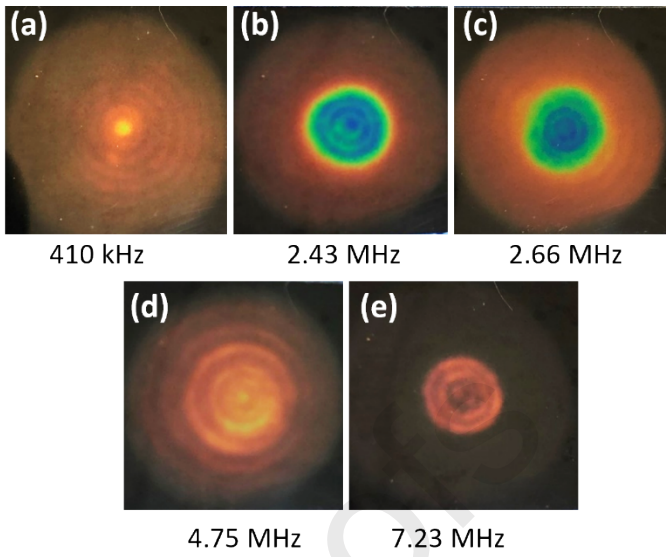

Figure 4: Visualisation of displacement of the higher vibrational modes of a flexural transducer (a-e) using thermochromic liquid crystal.

Resonances are clearly observed over a wide range of frequencies. For lower frequencies the correct number of rings are observed, while at higher frequencies the resolution of the film is limited by the thermal conductivity of the aluminium cap and thermal diffusion within the TLC sensor [31]. The smallest observable distance between two resolved antinodes in figure 5 is 1.2 mm, suggesting sub-mm resolution may be possible with these sensors. The switching speed of TLC sensor films can be as fast as milliseconds [15], and in our experiments the time until a suitable image is obtained is governed by the starting temperature of the transducer, the TLC film temperature sensitivity range, and the acoustic intensity for a given frequency (the amount of energy available for absorption that drives the local heating). The “on” and “off” times were 1-2 seconds (measured based on the video of switching; the video in real time is available as supplementary data).

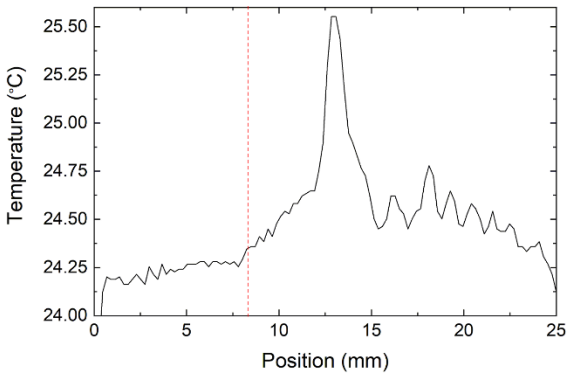

Figure 5: Temperature plot extracted from 720 kHz image excited at 2 V. No underlay to the left of the dashed line.

The mechanism behind the visualisation in the TLC sensor is thermal. All transducers heat up in operation, but the heating for the transducer used here is relatively uniform due to the very high thermal conductivity of the aluminium cap; this was shown in figure 4 of reference [12]. Such heating does not produce the patterns observed here. However, local absorption of ultrasound within the sensor (both the underlay and the TLC) leads to local heating, which can be observed by the change in colour of the TLC film. To confirm this effect, thermography was performed on the transducer without the TLC film. The transducer face was coated with black paint to ensure even IR emissivity, with a piece of elastic underlay film covering just over half of the transducer face. The result is shown in Figure 3(c), with the edge of the underlay marked by a dashed line; above the line (no underlay) the temperature is fairly constant, while the same series of bright rings are observed for the underlay (below the line). Figure 5 shows the temperature profile of the 720 kHz resonance for a line taken through the centre of the transducer, passing through a region with no underlay (above the dashed line) through the centre and to a region where peaks are observed. The transducer surface (no underlay) shows a very small amount of heating across the transducer face, but heat is produced in the underlay, with a maximum temperature rise of around 1.25°C at the centre. The series of peaks in temperature increase observed using this technique matches the ring positions observed using the TLC (figure 3(b)), confirming that the rings are caused by heating. Further heating will also occur in the TLC film, ensuring that the overall temperature rise is sufficient to change the colour of the TLC.

The heating observed in the TLC is a function of the frequency (wavelength) of the ultrasound, the displacement at the surface, the efficiency of ultrasound absorption (which is worse at higher wavelengths), and the chosen TLC temperature range and room temperature. TLCs are viscoelastic and effective absorbers of ultrasound, in particular at MHz frequencies. A frequency-dependence to the efficiency of the heating is expected; the longer the wavelength, the "thinner" the TLC film is relative to the wavelength, so less energy can be absorbed. The speed of ultrasound propagation in a typical LC is 1500 m/s [32]. At 1 MHz, the ultrasound wavelength in TLC is approximately 1.5 mm, while at 5 MHz it is 300 µm, and at 40 kHz it is 37.5 mm. Therefore sensitivity is expected to be higher for higher frequencies. However, the resonance amplitudes of the transducer drop off at higher frequencies (shown in figure 2), hence for this transducer the sensor shows the most thermal contrast for the 2-3 MHz modes.

Our previous work using PDLC sensors showed that clearing was efficient for frequencies over 2 MHz, but that for sub-MHz frequencies a very large displacement was required for clearing [12]. However, lower frequencies are used for some NDT applications, including frequencies from around 40 kHz for inspection of defects on the surfaces of plates and billets [33], and operation using just the TLC layer is not possible for such low frequencies due to the wavelength of ultrasound within the TLC. Previous researchers have used a layer of paraffin with a TLC paint to act as an absorbing layer to improve sensitivity [20]. In this work, the underlay takes the same role, allowing the sensor to be removable and reusable. Figures 3(b) and 4(a) show that the compound sensor works efficiently down to frequencies in the hundreds of kHz range, a significant improvement over the PDLC sensors.

In order to demonstrate operation at lower frequencies an alternative set-up was used, which offered large enough displacements at 40 kHz, and also enabled both in-plane and out-of-plane displacements to be detected. An ultrasonic horn was applied to a Perspex plate and standing Lamb waves were generated, with Perspex chosen due to its acoustic properties and low thermal conductivity. Figure 1(b) shows the measurement set-up used, with figure 6 showing the positioning of the horn and the standing wave pattern expected. The Perspex plate was 3 mm thick, and at this thickness the frequency-thickness product is very low: 0.12 MHz*mm. In this region only two Lamb wavemodes are supported: S_0 and a highly dispersive A_0. The horn was placed at approximately 49 mm from the sample edges, and moved around until a standing wave was obtained.

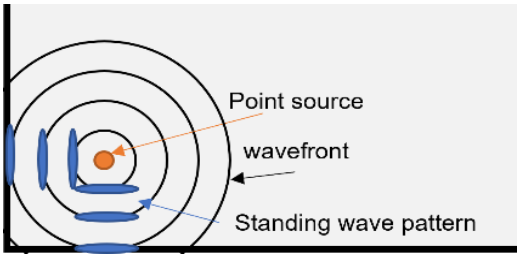

Figure 6: Measurement set-up for imaging Lamb waves in Perspex plate.

Figure 7 shows the results obtained once a standing wave was formed. The laboratory was at a higher temperature than is optimal for the TLC sensor, but a standing wave image was still obtained, shown as green stripes on a red background in figure 7(a). The image was processed and hue extracted for better visibility, with the processed results shown in figure 7(b). Despite the non-optimal experimental conditions, a standing wave

pattern can clearly be seen. By measuring the distance between peaks, a wavelength of 7mm ±1mm was estimated. This corresponds to the A_0 mode (velocity 280 m/s for Perspex), which is predominantly out-of-plane at this frequency·thickness. The edges of the sample, and a temperature increase measured outside of the sample edges, can also be seen. The mechanism behind the heating observed away from the plate is currently being investigated.

4. Conclusions

We have demonstrated the use of removable TLC-based sensors for visualisation of vibration over a broad frequency range, with operation demonstrated between 40 kHz and 7.23 MHz. The lateral resolution of the sensors allowed detailed characterisation of ring-like wavemodes on the face of a flexural air-coupled transducer, with resolution of at least 1 mm. The switching speed of the sensors is 1-2 seconds, with the exact timing dependant on the experimental arrangement, ultrasound power, and environmental factors. The speed of visualisation at much lower cost compared to vibrometry makes the new sensor attractive for use in condition monitoring, for fast assessment of transducer quality, or acoustic field distribution in power ultrasonic systems.

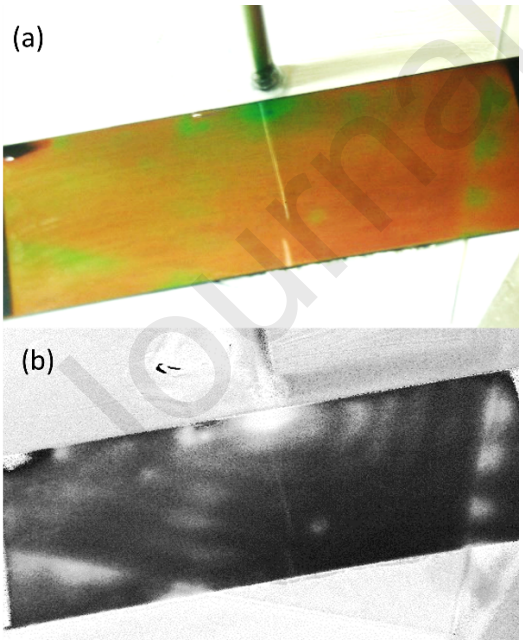

Figure 7: Visualisation of standing Lamb waves on a Perspex plate using TLC sensor, showing (a) green stripes on red background, (b) processed image extracting hue for better visibility.

The TLC based sensors do not require external power and will be compatible with robotic vision, with ongoing work focused on converting a photograph to a heatmap to quantify the temperature increase across the sensor, as an alternative to thermal imaging [30]. The suggested visualisation method is a fast and low-cost alternative to laser vibrometry, or could be used as an addition to vibrometry for quick tests, for example when choosing which area on the sample to scan. The suggested approach to ultrasound visualisation will be synergistic with thermosonics [34-36] – where defects are detected through local heating of a surface crack due to its edges rubbing together when excited by ultrasound. Thermography, which is widely used for defect detection in NDT, could also be performed using the same film sensor, without the need for a thermal camera. Alternatively, thermal imaging could be used for acoustic field imaging when the absorbing underlay is applied to a sample; however, this is at significantly increased cost compared to the TLC compound sensor.

The use of a compound sensor comprising TLC film plus an absorbing underlay allows operation at much lower frequency than has been obtained previously when using PDLC sensors. The temperature of operation is solely dependent on the choice of TLC and underlay materials, with high temperature inspection possible with suitable choices. Future work will aim to extend the frequency range of the technique by investigating sensitivity for different material choices, with the aim to push detection capabilities towards the audible range. The sensors offer significant promise for visualisation of different wavefields. Kagawa [19] has shown that in-plane displacement (shear waves) can be detected through the use of viscous couplant and heating due to rubbing inside the couplant. This is highly promising to develop further as shear waves are widely used in NDT, but are much more difficult to map with vibrometry, and a wavefield imaging technique that will work for purely in-plane motion will be of great interest.

Acknowledgements: This work was funded via the Research Centre in NDE (EPSRC EP/L022125/1). MT thanks FIND CDT for funding her PhD.

References:

[1] P Thayer, *"RCNDE industrial members' vision for the future requirements for NDE"*, Insight 54(3) 124 (2012)

[2] Y Yao, Y Pan, S Liu, *"Power ultrasound and its applications: A state-of-the-art review"*, Ultrasonics

Sonochemistry 62 104722 (2020)

[3] SJ Rothberg et al., *"An international review of laser Doppler vibrometry: Making light work of vibration measurement"*, Opt. Lasers Eng. 99 11-22 (2017)

[4] M Klun, D Zupan, J Lopatic, A Kryzanowski, *"On the Application of Laser Vibrometry to Perform Structural Health Monitoring in Non-Stationary Conditions of a Hydropower Dam"*, Sensors 19(17) 3811 (2019)

[5] H Xu, L Liu, X Li, Y Xiang and F-Z Xuan, *"Wavefield imaging of nonlinear ultrasonic Lamb waves for visualizing fatigue micro-cracks"*, Ultrasonics 138 107214 (2024)

[6] JS Sandhu and H Wang, *"Recent Advances in Acoustography-based NDE"*, in: Gdoutos, E.E. (eds) Recent Advances in Experimental Mechanics. Springer, Dordrecht (2002)

[7] PJ Collings and M Hird, *Introduction to Liquid Crystals: Chemistry and Physics* (1st ed.). CRC Press (1997)

[8] JS Sandhu, H Wang, WJ Popek and P Sincebaugh, *"Acoustography: a side-by-side comparison with conventional ultrasonic scanning"*, Proc. SPIE 3585 163-72 (2001)

[9] JS Sandhu, RW Schoonover, JI Weber, J Tawiah, V Kunin and MA Anastasio, *"Transducer Field Imaging Using Acoustography"*, Advances in Acoustics and Vibration 275858 (2012)

[10] GL Rodriguez, J Weber, JS Sandhu and MA Anastasio, *"Feasibility study of complex wavefield retrieval in off-axis acoustic holography employing an acousto-optic sensor"*, Ultrasonics 51 847 (2011)

[11] AS Chen, DP Almond and B Harris, *"Acoustography as a means of monitoring damage in composites during static or fatigue loading"*, Meas Sci and Tech 12(2) 151 (2001)

[12] O Trushkevych, TJR Eriksson, SN Ramadas, SM Dixon and RS Edwards, *"Ultrasound sensing using the acousto-optic effect in polymer dispersed liquid crystals"*, Applied Physics Letters 107, 054102 (2015)

[13] RS Edwards, J Ward, LQ Zhou and O Trushkevych, *"The interaction of polymer dispersed liquid crystal sensors with ultrasound"*, Applied Physics Letters 116, 044104 (2020)

[14] O Trushkevych, V Yu Reshetnyak, M Turvey and RS Edwards, under review.

[15] I Sage, *Thermochromic Liquid Crystals in Devices*, Chapter 5 Liquid Crystals — Applications and Uses, (Volume 3), Litton Systems Canada (1992)

[16] https://www.edmundoptics.co.uk/f/temperature-sensitive-liquid-crystal-sheets/11878/, Accessed 6-04-2023

[17] https://www.sfxc.co.uk/products/sfxc-sprayable-liquid-crystal-ink, Accessed: 6-04-2023

[18] D Cook and RE Werchan, *"Mapping ultrasonic fields with cholesteric liquid crystals"*, Ultrasonics 9(2) 101 (1971)

[19] Y Kagawa, T Hatakeyama and Y Tanaka, *"Detection and visualization of ultrasonic fields and vibrations by means of liquid crystals"*, J Snd and Vibr 36(3) 407 (1974)

[20] R Denis, *"Characterization of ultrasonic transducers using cholesteric liquid crystals"*, Ultrasonics 16(1) 37-43 (1978)

[21] ME Haran, *"Visualization and measurement of ultrasonic wavefronts"*, Proc IEEE 67(4) 454 (1979)

[22] J Sandhu, H Wang and WJ Popek, *"Acoustography for rapid ultrasonic inspection of composites"*, Proc SPIE 2944 1117 (1996)

[23] K Martin and R Fernandez, *"A thermal beam-shape phantom for ultrasound physiotherapy transducers"*, Ultrasound Med Biol 23 1267 (1997)

[24] IS Lopez, AL Mendonca and M Fernandes, *"Europium complex-based thermochromic sensor for integration in plastic optical fibres"*, Optical Materials 34(8) 1447 (2012)

[25] J Kim and M Kim, *"Focal position control of ultrasonic transducer made of plano-concave form piezoelectric vibrator"*, Ultrasonics 121 106668 (2022)

[26] I Butterworth, J Barrie, B Zeqiri, G Zauhar and B Parisot, *"Exploiting Thermochromic Materials for the Rapid Quality Assurance of Physiotherapy Ultrasound Treatment Heads"*, Ultrasound Med Biol 23 1267 (1997)

[27] S Ambrogio et al, *"A polyvinyl alcohol-based thermochromic material for ultrasound therapy phantoms"*, Ultrasound Med Biol 46(11) 3135 (2020)

[28] TJR Eriksson, SN Ramadas and S Dixon, *"Experimental and simulation characterisation of flexural vibration modes in unimorph ultrasound transducers"*, Ultrasonics, 65 242-248 (2016)

[29] JL Rose, *Ultrasonic Waves in Solid Media*, Cambridge University Press (1999)

[30] M Turvey, O Trushkevych, DJ McKnight and RS Edwards, under review.

[31] M Eames et al., "*Low-Cost Thermochromic Quality Assurance Phantom for Therapeutic Ultrasound Devices: A Proof of Concept*", Ultrasound Med Biol 49(1) 269-277 (2023)

[32] AV Glushchenko, VS Sperkach and OV Yaroshchuk, *"Sound Propagation in Liquid Crystal 5CB and 5CB Based Aerosil Suspensions"*, Int J of Fluid Mechanics Research 30(3):299-306 (2003)

[33] L Xiang, D Greenshields, S Dixon and RS Edwards, *"Phased electromagnetic acoustic transducer array for Rayleigh wave surface defect detection"*, IEEE Transactions on Ultrasonics, Ferroelectrics, and Frequency Control, 67(7) 1403-1411 (2020)

[34] M Vollmer and K-P Mollmann, *Infrared Thermal Imaging*, Wiley (2017)

[35] G Bolu, A Gachagan, G Pierce and G Harvey, *"Reliable thermosonic inspection of aero engine turbine blades"*, Insight 52 (9) 488 (2010)

[36] U Polimeno, DP Almond, B Weekes and EWJ Chen, *"A compact thermosonic inspection system for the inspection of composites"*, Compos B: Eng 59 67 (2014)

Acoustic field visualisation using local absorption of ultrasound and thermochromic liquid crystals

Authors: O Trushkevych, M Turvey, DR Bilson, R Watson, DA Hutchins and R.S. Edwards

- A passive sensor for ultrasound based on thermochromic liquid crystals (TLCs) is introduced.
- Its use for characterising ultrasound sensors and for visualising wavefields in plates is presented and explained.
- The sensor offers the potential for immediate visualisation without the need for scanning, and can be applied directly onto a sample or in air. No water bath is required.
- Ultrasound is visualised via local heating of the TLC and an absorbing backing layer.

Declaration of interests

☐ The authors declare that they have no known competing financial interests or personal relationships that could have appeared to influence the work reported in this paper.

☒ The authors declare the following financial interests/personal relationships which may be considered as potential competing interests:

Dave Hutchins, Oksana Trushkevych reports financial support was provided by UK Research Centre in Non-Destructive Evaluation. Rachel Edwards, Oksana Trushkevych has patent #PCT/GB2022/052279 pending to University of Warwick. R Edwards is on the editorial board for this journal. If there are other authors, they declare that they have no known competing financial interests or personal relationships that could have appeared to influence the work reported in this paper.